Monitoring ageing in beef samples using surface wave elastography: a feasibility study

Nicolás Benech[1*], Sofía Aguiar[2], Gustavo A. Grinspan[1,3]

[1]Laboratorio de Acústica Ultrasonora, Facultad de Ciencias, Igua 4225, 11200, Montevideo, Uruguay

[*]nbenech@fisica.edu.uy

[2]Intstituto de Ensayo de Materiales, Facultad de Ingeniería, J. Herrera y Reisig, 565, Montevideo, Uruguay

[3]Sección Biofísica y Biología de Sistemas, Facultad de Ciencias, Igua 4225, 11200, Montevideo, Uruguay

Abstract.

The maturation process of beef improves meat quality. Several bio-physical-chemical changes occur during ageing. Often, they emerge macroscopically as variations in the mechanical properties of the tissue. Most of the actual testing methods are destructive. Therefore, the number of tested samples is limited.Elastography was born as a medical imaging modality to estimate noninvasivelythe elasticity of soft tissues. Thus, its application to monitorageingcould help to overcome some drawbacks of destructive methods. However, its use is minimum in industry. In this work, we study the feasibility of using surface wave elastography (SWE) to monitor beef ageing.We tested 25 samples for 21 consecutive days. The results show a decay close to 50% in thes hear elasticity of all samples. In addition, the rate of decay show that the elasticity reduction is greater in the first days for most samples.These results are consistent with previous knowledge in this area, which encourages further research to improve the method and increase its performance and reliability.

Keywords: ageing, elastography, surface waves, mechanical properties

1. Introduction

To obtain meat of high quality, post-mortem ageing at 4ºC or lower for a certain period is required. Tenderness and flavor are improved during this period becausebiochemical and physicochemical processes occur during post-mortem ageing [1-2]. These processes include the increase of membrane water permeability and the weakening of connective tissue [3]. Thus, it is not surprising that ageing causes changes in the mechanical properties of meat. These changes are evidenced by tensile tests [4], shear force tests [5] or texturometers [6].All these methods share the disadvantage that they are destructive and therefore the samples tested lose their commercial value. In

addition, it is not possible to monitor the changes of a single piece at arbitrary time intervals. Thus, one challenge facing the industry is to account with a reliable and non-destructive method to estimate the mechanical properties of meat during post-mortem ageing.

Ageing periods are usually more than 10 days for beef [7]. However, there is no agreement on which is the best ageing time before commercialization, since there is a large variation in both the rate and extent of post-mortem tenderization depending on the muscle type and processing conditions [8].It has been reported that different muscles from the same carcass respond differently to the same ageing period [9]. Moreover, there exist contradictory reports even for the same muscle. Some studies in longissimus dorsi for example, found that there is little difference in shear values after 7 days ageing [10]. However, other studies reported considerable tenderization for the same muscle and in the same time period [11].Thus, a method for noninvasive monitoring the mechanical properties of beef samples could benefit the industry in decision making on ageing periods and commercialization.

Elastography was born as a medical imaging modality to estimate the local elasticity in soft tissues [12]. The goal is to improve the medical diagnosis of those pathologies which affect the mechanical properties of some tissues. Examples include breast tumor or liver fibrosis [13]-[14]. Within the past 30 years, several methods and techniques were proposed including static and dynamic methods [15]-[17]. Most of them are ultrasound-based techniques, due to the availability and portability of ultrasound scanners. Despite the spreading of elastography in the medical field, its use has been little studied in the food industry as a whole and particularly in beef industry.

Previous works including (static) elastography to study meat quality characteristics of pork showed that elastographic results are significantly correlated to shear force tests [18]. Dynamic elastography methods (transient elastography) were able to quantify the viscoelasticity [19] and anisotropy [20] of beef samples. In addition, it showed a linear correlation with pH during rigormortis [21]. However, none of those methods was translated into devices for industrial use. We believe that this fact is due to the need foradapted ultrasound scanners and highly specialized personnel to operate them. In addition, none of these methods is easily adapted to the production line.

Surface wave elastography (SWE) is an emerging elastographic method. Applications include estimating the elasticity of soft tissues *in vivo* [22]-[23],the elasticity of tendons *in vivo* [24] and even the elasticity of fruits [25]. The goal in SWE

is to estimate bulk elastic parameters from waves propagating at the surface of the sample. Unlike the ultrasound-based methods mentioned above, SWE does not intend to image the elasticity of tissues. Instead, it brings a mean value of their elasticity in a region of interest (ROI). Therefore, SWE methods use simpler algorithms and measuring devices. Consequently, the associated costs are lower, and the final user requires a minimal training. Thus, SWE is a good candidate to monitor changes of mean elasticity within a ROI in tissues as a function of time, temperature, environmental conditions, etc.

In this work, the main objective was to study the feasibility of using surface wave elastography as a method to monitor the ageing process of beef samples. Recently, we have developed a SWE device and method to estimate the elasticity of isotropic and transversely isotropic tissues [26]. We named this method as *non-ultrasound surface wave elastography* (NU-SWE). Using this device, we tested five hindquarter cuts during 21 consecutive days in order to study if the NU-SWE method is able to follow the changes in their shear elasticity and provide information about its decay rate.

2. Materials and methods

2.1 Surface wave elastography

In this section, we briefly describe the NU-SWE method employed in this study. Details about the device and theory of operation can be found in [26],[27].

The goal in NU-SWE is to estimate bulk shear elastic modulus from surface wave measurements within a ROI. The challenge is to find the relationship between the surface wave speed $V_s$and the bulk shear wave speed V_b because the laterhas a simple relation with the shear elastic modulus $\mu = \rho V_b^2$ [28]. In this expression ρ represents the material density of the beef sample and a lossless elastic medium is assumed. The relationship between V_s and $V_b$is obtained via a physical model for surface wave propagation. Skeletal muscle is an anisotropic tissue. The orientation of muscle fibers defines a symmetry axis. The elasticity is isotropic within a plane perpendicular to fibers. Thus, skeletal muscle is assumed as a transversely isotropic tissue [20]. Therefore, there are two elastic constants related to shear wave propagation. $\mu_\perp = \rho(V_b^\perp)^2$is the elastic constant related to the shear wave propagating perpendicular to the fibers with perpendicular polarization and$\mu_\parallel = \rho\left(V_b^\parallel\right)^2$is related to the shear wave propagating along the fibers direction with perpendicular polarization.

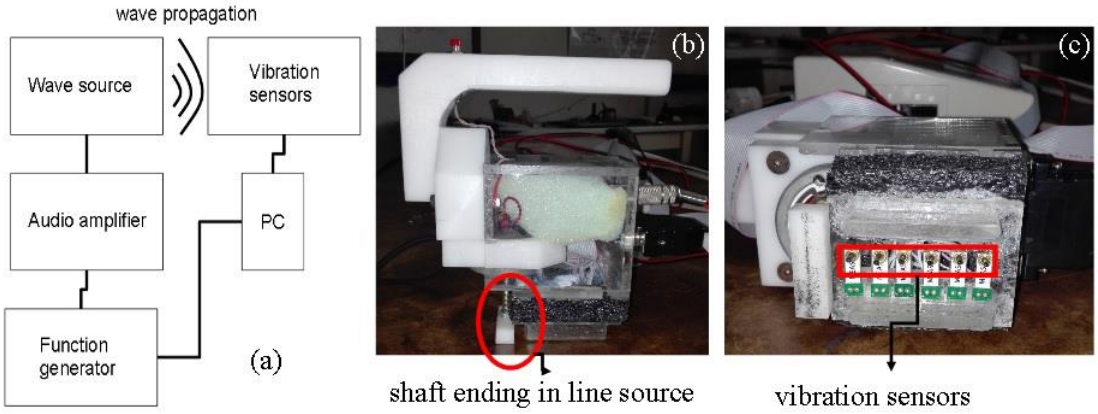

Figure 1. (a) Schematic diagram of the NU-SWE device. The PC controls the function generator and the vibration sensors.(b) Side view of the prototype device. The shaft ending in a linear source is highlighted. (c) Bottom view of the prototype. The piezoelectric vibration sensors are highlighted.

As is shown in figure 1, the main components of the NU-SWE device are the wave generator and the vibration sensors. The wave generator is a vibrator with a shaft attached to it, ending in a linear source. The source vibrates normally to the free surface of the sample. If it is oriented perpendicular to the muscle fibers, it excites a wave that propagates along the fibers with perpendicular polarization. The vibration sensors are piezoelectric levers (bimorphs). They generate a voltage when deflected. A mass attached to the levers offers sensitivity in the frequency range used in our experiments (150 – 200 Hz). We use 6 sensors at known positions along the surface to record the surface vibrations. By computing the phase difference between signals, we obtain the phase speed of the surface displacement fieldV_S. Figure 2(a) shows the device being applied to a sample of bottom round. In this sample, the muscle fibers are oriented mainly along the longitudinal axis. The linear source acts perpendicular to the fibers and the sensors record the displacement field along the fibers' direction. Figure 2(b) displays the field recorded by each sensor, where the time-shift between them is clearly visible.

Within soft tissues, a critical distance exists where only surface waves propagate, without contribution from reflected waves from the opposite surface [27]. The different surface wave types interfere with each other on the surface. Therefore, the phase speed of the recorded displacement field is dispersive. The dispersion relation depends on the value of the bulk shear wave speedV_b. Using a fitting algorithm based on least squares, the shear wave speed is retrieved. For the orientation of the linear source, the value of $V_b^{//}$ is retrieved. If the material density ρ is known, our device allows

computing $\mu_{//}$. We note here that the linear source can also be oriented parallel to the fibers. This way, $\mu_{\perp}$ could also be measured. However, we choose to measure only $\mu_{//}$ because this value would be comparable to other methods like shear force tests. The relationship between V_s and V_b is depicted in the appendix.

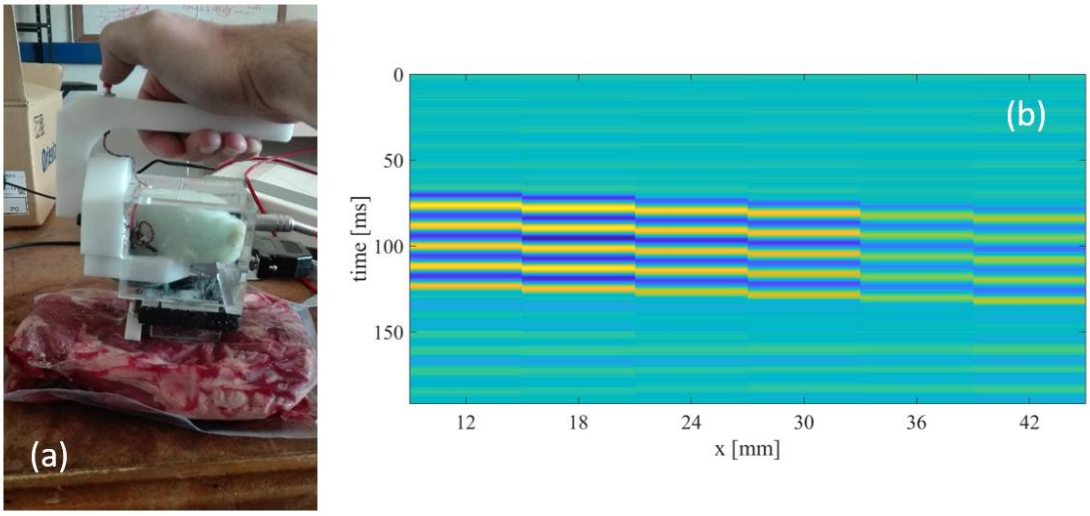

Figure 2.(a) Example of application of the device over a sample of bottom of round. The linear source is aligned perpendicular to the muscle fibers. (b) Vibration field recorded by the sensors. The time shift between sensors is clearly seen.

The "sensing" depth of the surface wave is related to its wavelength. In our experiments, we use frequencies in the range 150-200 Hz. Typical values of the shear wave speed in beef samples are between 3 and 8 m/s. Thus, the wavelength varies between 1.5 and 5 cm. These values are much larger than the plastic film bags used for vacuum sealing. In previous works [29], we tested the device with "naked" beef samples. Then, the samples were vacuum sealed and tested again. The measurement of the shear elasticity was unaltered by the plastic bag. Thus, our device not only is nondestructive, but the beef samples can be tested without even touching them, preserving the sanitary conditions in a slaughterhouse.

2.2 Shear Wave Elastography

The surface wave method described above estimates the bulk shear elasticity of the beef sample from surface sensors. In order to compare the estimated value with an independent reference method, we used an Aixplorer V12 (SuperSonic Imagine, Aix-en-Province, France). This device remotely generates a shear wave in the bulk of the

sample, via acoustic radiation force, and tracks its propagation speed in real time using ultrafast frame rates. The method is termed as supersonic shear imaging (SSI) [30]. The screen displays a 2D image of the shear elasticity (in kPa), within the selected ROI. Figure 3 displays images of the experimental setup. We used a linear array probe (SL 10-2) with a 2-10 Mhz bandwidth which allows elasticity imaging up to 4 cm depth. The sample is a piece of bottom round from a local butcher shop. Its approximate dimensions (large×width×depth) are 18×5×6 cm^3. The array is positioned parallel to the muscle fibers. Therefore, the shear wave propagation is parallel, and the polarization is perpendicular to the muscle fibers. Thus, both the surface and bulk methods estimate $\mu_{//}$.

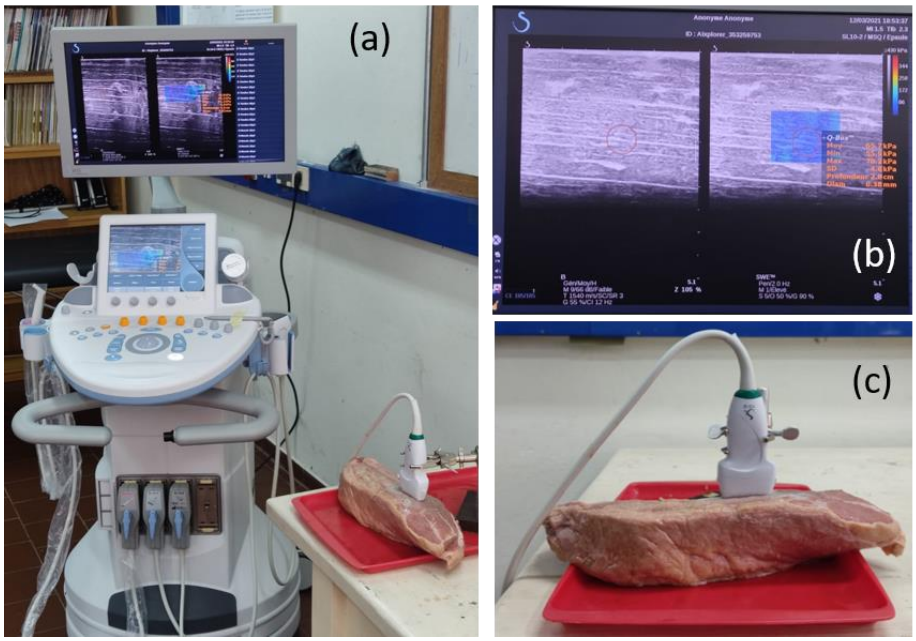

Figure 3. Experimental setup for shear wave elastography measurements. (a) The AixplorerV12 device and the linear array over a sample of bottom round. (b) Detail of the screen of the Aixplorer device. The screen displays two images. On the left, a sonogram of the sample where the fiber orientation is clearly seen. On the right, the elasticity map is superimposed to the sonogram in the ROI. (c) Detail of the array positioned over the beef sample. The array is positioned parallel to the muscle fibers.

2.3 Sample preparation and ageing conditions

In this work, a total of 25 beef samples were analyzed. The batch consistedof 5 samples of 5 different beef cuts: strip loin (SL), thick flank (TF), tail of rump (TR), eye of round (ER) and bottom round (BR). The samples were provided by a local slaughterhouse. All samples came from animals of the same breed, gender, age and type of feeding. They were vacuum sealed and arrived at our laboratory after three days post-mortem and were kept in a cold chamber at 0ºC. The cold chamber is spacey enough to

allow performing the experiments inside it as shown in figure 4. Nevertheless, due to door opening and varying external conditions, we registered temperature fluctuations (between 0 ºC and 3 ºC) during the experiments.

Figure 4.(a) Cold chamber with beef samples inside. (b) The tests were performed inside the cold chamber.

Ten measurements were performed in each sample per day. All samples were measured every day during 21 consecutive days. In the first day of experiments, the ROI was marked in the plastic bag. This way, we ensured that the experiments were carried out within the same ROI.

2.4 Statistical analysis

For comparison between the surface wave and the bulk shear wave measurements acquired with the NU-SWE and SSI, respectively, we performed a Bland-Altman plot [31] and analyzed the mean difference using the one sample t-test [32].

Regarding the ageing process, we performed the Welch's *t*-test [32] to test the hypothesis of two cut types have equal meanof the shear elastic modulus at the end of the measurements. We used the set of fifty measurements for each cut type to test the hypothesis (ten measurements per sample and five samples for each cut type). We also tested the hypothesis of the same cut type have equal mean before and after the 21-day ageing process.

Our data allow studying the rate of decay of the shear modulus by computing locally the slope of the shear modulus curve as a function of time. We performed a one-way ANOVA [32] to compare the slope values intra samples of the same cut type. In addition, we tested the hypothesis that each cut type has an equal mean of the slope before and after the process.

In all cases we used a level of significance $p = 0.05$.

3 Results

3.1 Comparison between surface and bulk methods

Before beginning the ageing monitoring, we performed measurements on a single sample of bottom round, in order to compare the surface wave method with the shear wave method. The sample was acquired in a local butcher shop and kept at 4ºC for 24 hs before measurements.

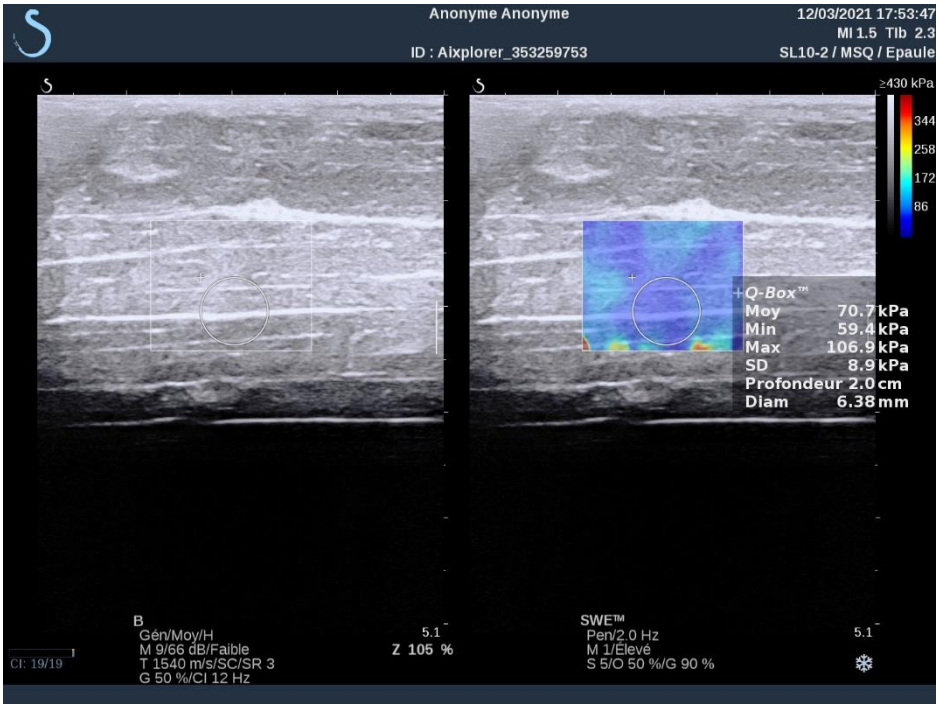

Figure 5. Screen capture of the Aixplorer V12 device while measuring the shear elasticity of a beef sample. The left image is a sonogram of the sample where the fiber orientation is clearly seen. The right image shows the superimposition of the elasticity map on the sonogram.

For the surface wave measurements, we marked 3 different ROIs on the surface of the sample and performed a set of 5 measurements in each ROI, totaling 15 measurements. The result was $V_b = 8.1 \pm 0.6$ m/s, where the uncertainty represents one standard deviation over the 15 measurements. Assuming a material density $\rho = 1.0 \times 10^3$ kg/m^3, the estimated shear elasticity was $\mu_{//} = 65.6 \pm 9.7$ kPa.

For the bulk shear wave measurements, we used the Aixplorer V12 with the musculoskeletal preset. Figure 5 displays a screen capture of the Aixplorer device during the experiments. The image is split in two. The left side is a sonogram (B mode) of the sample, where the fiber orientation is clearly visible. The right side shows the superimposition of the elasticity map on the sonogram. The white circumference is the selected ROI for which the mean shear elasticity value is displayed. The box also displays the measuring depth, the standard deviation, and the minimum and maximum values within the ROI. We repeated this procedure in 15 different positions in the volume of the sample while positioning the ultrasonic probe at the marked ROIs of the surface wave measurements. The estimated shear elasticity is $\mu_{//} = 69.2 \pm 8.4$ kPa.

Figure 6 displays the Bland-Altman plot comparing the surface and bulk methods. The mean difference was 1.42 kPa, higher on the bulk method. The standard deviation of the difference was 6.3 kPa. There were no data points out of the confidence interval, showing there was no influence of outliers. The one sample t-test of the mean difference indicated that it did not differ significantly from 0 ($p > 0.4$).

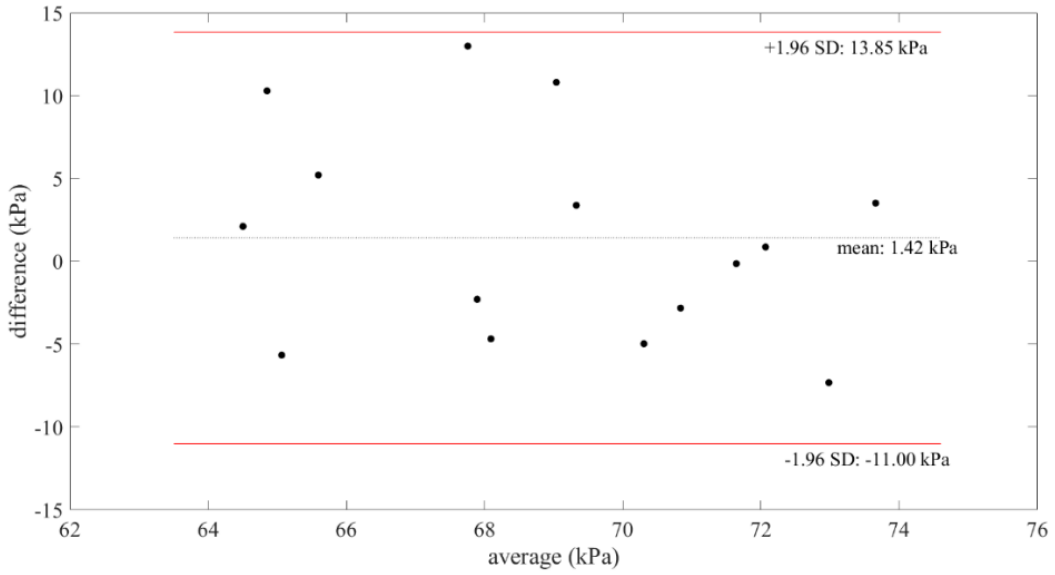

Figure 6. Bland-Altman plot comparing the data of the surface wave and the shear wave methods. The black dotted line indicates the mean value of the difference and the red lines indicate the 95% confidence interval (1.96 SD).

3.2 Monitoring ageing with surface wave elastography

Figure 7 displays the mean shear elastic modulus $\mu_{//}$ for each cut type as function of the maturation time measured with the surface wave method. The mean for each cut type is computed using the mean of each sample over the ten measurements.

The bars in this plot indicate one standard deviation. After initial fluctuations, a systematical decrease in the elastic modulus can be observed for all cut types. Some of them reach an almost constant elastic modulus well before the 21 days of ageing while others continue decreasing until the end of measurements.

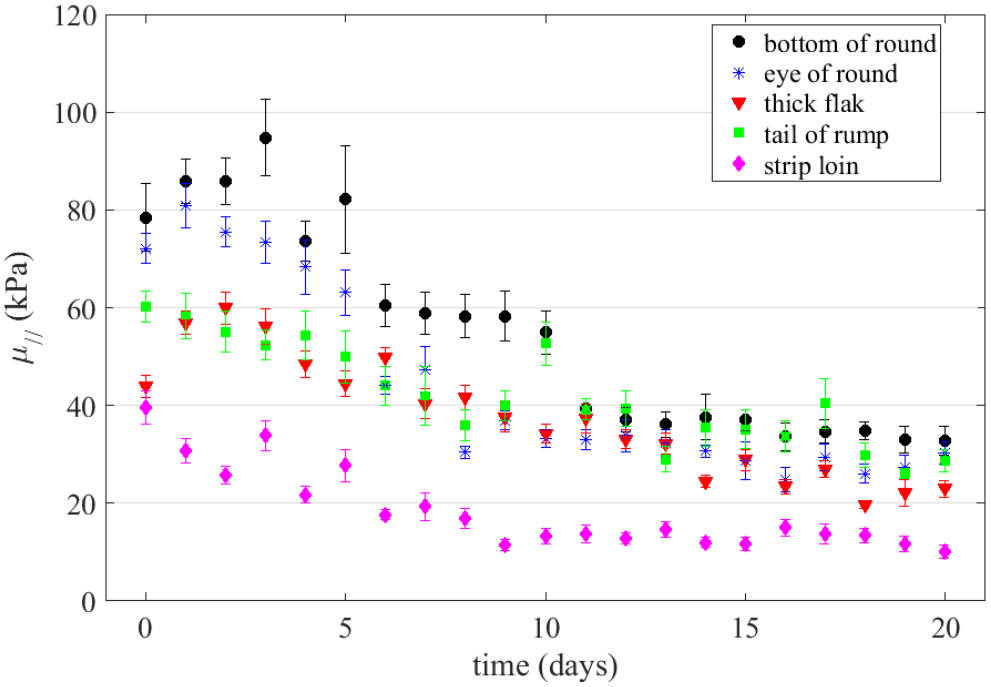

Figure 7. Mean elastic modulus for each cut type as function of the maturation time. The errorbar represents one standard deviation over the 5 samples for each cut type.

4. Discussion

The results displayed in figure 7 show that all the cut types studied here achieve a significant variation in their shear modulus after ageing ($p < 0.01$ in all cases). The decrease in $\mu_{//}$ is of the order of 50% compared to the initial values. They agree with those reported in other studies where it was found that ageing times between 8 and 14 days is enough for most cut types to achieve constant values of their mechanical properties [9]. However, we emphasize that the method used here is nondestructive and the samples do not lose their commercial value.

When comparing the cut types studied here, the results show that there is no significant difference in the shear elastic modulus of ER, BR and TR ($p > 0.3$). On the other hand, the elasticity of SL and TF have a significant difference between them ($p < 0.01$) and with all other cut types ($p < 0.001$ and $p < 0.01$ respectively).

Regarding the ER, the TR and the BR, these three cut types are located on the external and posterior face of the leg. Particularly, the ER is in the posterior face of the

thigh and the primary muscular plane that comprises it is the semitendinosus muscle. The TR is located on the external face of the thigh region, and its primary muscular plane is the biceps femoris muscle. On the other hand, the BR is a piece that is comprised between the ER and the TR. Thus, it is located on the external and posterior face of the thigh region, and its main muscular planes are the biceps femoris and semitendinosus muscles[33]. Therefore, from this point of view, it makes sense that the elasticity values of these cuts have not reflected significant differences between them.

The TF is also located in the thigh region, but its location is different from that of the ER, BR and TR. The TF is in the anterior face of the thigh, being its primary muscle plane the femoral quadriceps muscle [33]. Therefore, although TF also belongs to the thigh region, it is much less interrelated, both regionally and functionally, with the ER, BR and TR. It is therefore reasonable that the measurements of shear elasticity would be significantly different between these cut types and TF.

SL is located away from the thigh. It is in the region of the lumbar back and the muscular planes that compose it are mainly the illiocostalis, longissimus dorsi, multifidus dorsi and serratus dorsalis muscles (according to distance of the cut from the eye muscle) [33].From a functional point of view, these muscles act in the posture maintenance, unlike the muscles mentioned above which are related to locomotion. Thus, it is not surprising that the shear elastic modulus is significantly different between SL and all other samples. This result agrees with previous works which conclude that the tenderness of beef samples is correlated to their anatomical location. [34]-[36]. Among other factors, this is related to the distribution of different fiber types due to the muscle role in the live animal, which influences its mechanical properties. The muscles involved in posture are more oxidative than those involved in movement [37], [38].

The rate of change of the shear modulus is a property of interest for industry because its value allows describing the ageing time for each cut type. In addition, it could be coupled with other factors for decision making about the commercialization times and therefore affects the commercialization value.

When taking the derivative of the data displayed in figure 7, the result is noisy, and conclusions are hard to take. This is because the derivative operation amplifies the noise of the original data [39]. The uncertainty in our data came from different sources. Prior to the study reported here, a set of measurements were performed in order to estimate the incidence on the uncertainty of the inherent electronic noise and the algorithm that computes the surface wave speed. We took 5 hindquarter samples

(different from those of the aging study) and performed 64 measurements on each one. They were performed in a single day and under the same conditions of temperature, applied stress and the device's position over the sample. The applied stress was controlled by placing the device on a mechanical arm coupled to a stepper motor. A strain gauge at the bottom of the device allows measuring the applied stress. Under these controlled experimental conditions, the standard deviation represents between 0.5% and 1% of the mean value in all cases depending on the cut type.

Other sources must be added when tracking the samples over time. Ideally, the samples should all be measured under the same conditions of the controlled experiments mentioned above, regarding mainly the temperature and applied stress (i.e., the pressure exerted over the sample). However, as mentioned before, there are temperature fluctuations due to door opening and varying external conditions. In addition, as measurements were made freehand as shown in figure 4(b), the applied stress conditions are not necessarily the same in each measurement. The boundary conditions affect the internal stress of the sample and, as a consequence, the surface wave speed value.When the device is manually operated, the strain gauge avoids sharp variations in the boundary conditions. Nevertheless, it is not possible to ensure constant external pressure for each measurement. Therefore, the final uncertainty is greater than the obtained in the controlled experiments. In future versions of the device, we will address this issue. Finally, due to the small number of samples for each cut type, the influence of the variations of a single sample on the average is relevant.

One way to filter out the noise amplification in the time derivative operation is to take larger time steps to compute the difference of the shear elastic modulus. We took a time step of five days to compute the derivative. The result of this operation is displayed in figure 8 for each cut type. The rate of change decreases as a function of time.

We performed the one-way ANOVA analysis intra sample at the beginning and at the end of measurements. For each time interval, the results show that there is no significant difference in the slope of the shear elastic modulus between samples of the same cut type ($p > 0.3$ in all cases). This result is consistent with the origin of the samples used in this study, where all belong to the same breed, age, gender and feeding type. It is known that the mechanical properties depend on all these parameters [8],[9]. Our research does not include yet these variables, but this point will be addressed in future works.

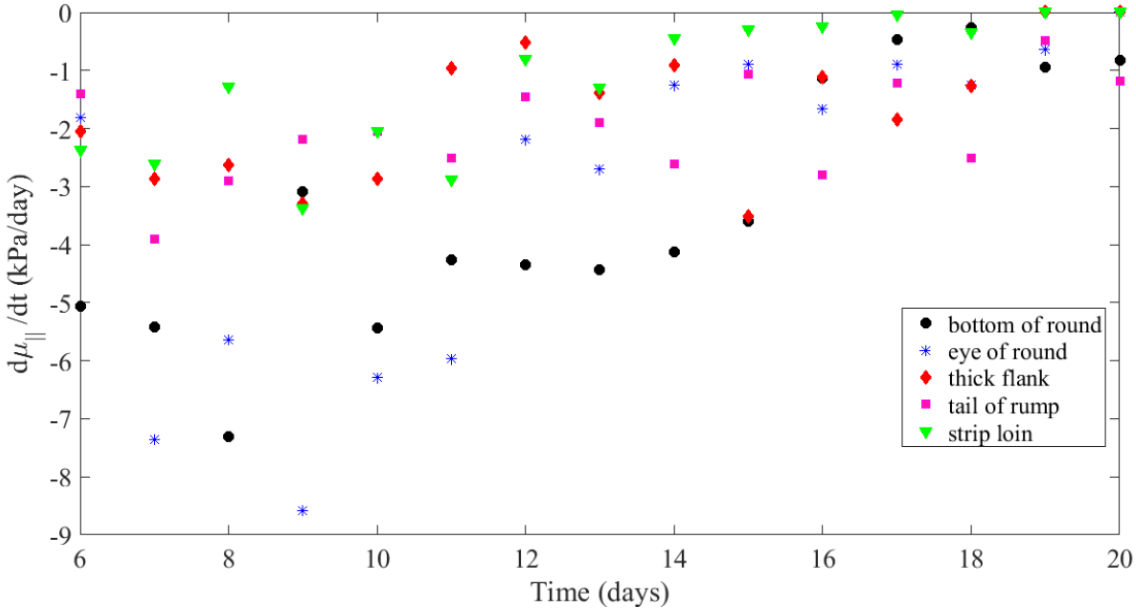

Figure 8. Rate of change of the shear modulus for different cut types.

The statistical analysis show that the slope at the end of measurements is significantly different from the initial slope ($p < 0.03$) for all cut types, except for the TF ($p > 0.3$). Indeed, the rate of decay for TF has not significant differences throughout the whole period, meaning that its shear modulus decreases with the same rate. Presumably, this sample will continue to decrease its elasticity value beyond the 21 days covered by this study. The number of samples should be increased to know if this is a casuistic result found in this work or if it is a characteristic behavior of this cut type.

For the other cut types, we tested the hypothesis of the final slope be equal to the slope at previous days. The results show that the slope of the SL does not differ significantly from itself from day 13 onwards ($p > 0.7$).Regarding the ER, BR and TR, their slope remains unchanged from day 14($p > 0.4$), 18 ($p > 0.5$) and 16 ($p > 0.5$) respectively. Thus, the results show that the cut types analyzed in this work have different maturation times. This agrees with previous studies showing that different muscles need different maturation times to reach minimum values in shear force tests [40].

5. Conclusion

To the best of our knowledge, this is the first time that surface wave elastography is employed in monitoring the mechanical properties of beef samples during aging. The NU-SWE method used in this study assumes that the beef is a lossless elastic medium. Thus, the only mechanical property monitored was the shear

elasticity. We performed a comparison between the surface wave method and a bulk shear wave method on a single sample. The results show good agreement between them although it is necessary to increase the number of samples in the study to provide more reliable results.

The results show that, after 21 days of ageing time, the samples achieve a significant reduction of their shear elasticity. The reduction is close to 50% for all samples. In addition, we show that the shear elasticity of the cut types studied is different depending on the functionality of the muscle in the live animal.

Regarding the rate of change of the shear elasticity, the results show that the slope is greater in the first days of ageing. It decelerates at the end of measurements. The SL is the first to reach a constant decaying rate after 13 days of maturation. The other cut types require a longer time. The behavior of the TF is different. Its shear elasticity decreases at the same rate throughout the whole period covered.

The results reported here are reasonably well consistent with previous knowledge in this area, considering that there is no general agreement about the maturation time required for beef samples or about the rate of change in their mechanical properties. Nevertheless, the surface wave elastography device needs improvements in order to reduce the uncertainty on the measurements when operated freehand.

Acknowledgments

We thank Patricia Lema for letting us use the coldchamber at her lab in the Engineering Faculty and Rafael Piriz for providing us the beef samples. We also thank Project ANII FMV_1_2019_1_155527 for let us use their Aixplorer device. This work was supported by Comisión Sectorial de Investigación Científica(CSIC, Uruguay) and by ITP Ltd.

Appendix

Guided wave propagation in finite plates takes place after reflection back and forth on the bounded surfaces. Often, reflections give birth to mode conversion between P and SV waves which generate a complicated pattern of interference within the plate and dispersion curves for each mode with their respective cutoff frequency. However, due to the difference in orders of magnitude on the speed of P and S waves in soft tissues, there is no mode conversion [27]. In addition, due to the dipole characteristic of

the line source for shear waves, most part of the energy is carried in a specific angle which depends on the symmetry of the tissue [26].

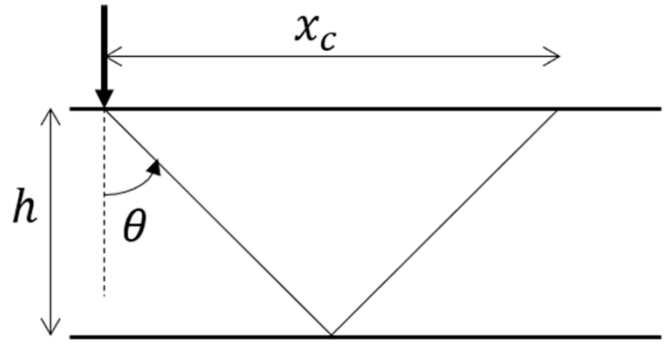

Figure A.1 Schematic representation of wave propagation in soft tissues. Within the volume of the sample, most part of the energy is carried as an SV wave which propagates in a specific angle with respect to the source direction. Consequently, there exists a distance x_s on the surface where only surface waves propagate.

Figure A1 shows schematically this situation. There exists a distance $x_c = 2h\tan(\theta)$ over the surface of the sample where only surface waves propagate. For transversally isotropic solids, like skeletal muscle, $\theta \cong 60º$. The mean depth in our samples is h =4 cm. Therefore, the distance $x_c \cong$ 12 cm. Thus, for $0 < x < x_c$, the vertical displacement of the surface is composed by the interference of the Rayleigh and the leaky surface wave: [27], [40].

$$u_z(x,t) = A_R\left[e^{-ikx} + A_L e^{-\zeta x} e^{-iqx}\right]e^{i\omega t} \text{(A. 1)}$$

where A_R is the amplitude and k the wave number of the Rayleigh wave, A_L is the relative amplitude between the leaky wave and the Rayleigh wave, $\zeta$and q are the imaginary and real parts of the leaky wave wavenumber, respectively. The phase $\phi(x)$ of the quantity between brackets is $\phi(x) = \text{atan}(N(x)/D(x))$ where:

$$N(x) = -\left[\sin(kx) + A_L e^{-\zeta x}\sin(qx)\right] \text{(A. 2)}$$

$$D(x) = \cos(kx) + A_L e^{-\zeta x}\cos(qx) \text{ (A. 3)}$$

The phase speed is, therefore:

$$V_s(\omega) = \omega\left(\frac{\partial\phi}{\partial x}\right)^{-1} = \omega\left[\frac{D^2 + N^2}{N'D - ND'}\right] \text{(A. 4)}$$

After some computation, the expression for the phase speed is:

$$V_s(\omega) = \frac{\omega}{k}\left\{\frac{1 + A_L^2 + 2A_L\cos\big((k-q)x - \epsilon\big)}{1 + A_L\left[(\chi+1)\cos\big((k-q)x-\epsilon\big) + \left(\frac{\delta}{k}\right)\sin\big((k-q)x-\epsilon\big) + \chi A_L\right]}\right\} \quad (A.5)$$

where $\chi = q/k, \delta = \zeta k$, and$\epsilon$ is a phase constant between the Rayleigh and leaky waves. Experimentally, we measure the phase speed of the surface wave within the frequency bandwidth of the source. The experimental curve is fitted, in a least squares sense, with the theoreticalphase speed computed from equation (A.5).Thus,V_b is obtained as the value which produces the best fit.

References

[1] K. Takahashi, "Structural weakening of skeletal muscle tissue during post-mortem ageing of meat: The non-enzymatic mechanism of meat tenderization", Meat Science 43, No. S, S67-S80, (1996).

[2] E. H. Lonergan, W. Zhang and S. M. Lonergan, "Biochemistry of post-mortem muscle. Lessons on mechanisms of meat tenderization", Meat Science 86, 184-195, (2010).

[3] C. E. Byrne, D. J. Troy and D. J. Buckely, "Post-mortem changes in muscle electrical properties of bovine M-longissimus dorsi and their relationship to meat quality attributes and pH fall", Meat Science, 54, 23-34, (2000).

[4] M. C. Lanari, A. E. Bevilacqua and N. E. Zaritsky, "Changes in tenderness during aging of vacuum packaged beef", J. Food Processing and Preservation, 11 (2), 95-109, (1987).

[5] C. L. Bratcher, D. D. Johnson, R. C. Littell and B. L. Gwartney, "The effects of quality grade, aging and location within muscle on Warner-Bratzler shear force in beef muscles on locomotion", Meat Science, 70, 279-284, (2005).

[6] K. Palka, "The influence of post-mortem ageing and roasting on the microstructure, texture and collagen solubility bovine semitendinosus muscle", Meat Science, 64, 191-198, (2003).

[7] J. Lepetit and J. Coulioli, "Mechanical properties of meat", Meat Science, 36, 203-237, (1994).

[8] D.L. Hopkins and G.H. Geesink, "Protein degradation post-mortem and tenderization" chapter 8 of "Applied muscle biology and meat science"Edited by M. Du and R. J. McCormick, CRC Press, Boca Raton, FL, (2009).

[9] M. Stuby-Souva, "Tenderness and ageing response of beef muscles of different quality grades before and after freezing", Doctoral dissertation, Oklahoma State University, Chap 2, (1994).

[10] R. Field, “Effect of castration on meat quality and quantity”, J. Animal Science, 32, 849-858, (1971).

[11] M. Koohmaraie, S. Seideman, J. Schollmeyer, T. Dutson and A. Babiker, “Factors associated with the tenderness of three bovine muscles”, Food Science, 53, 407-410, (1988).

[12] J. Ophir, I. Céspedes, H. Ponnekanti, Y. Yazdi and X. Li, “Elastography: A method for imaging the elasticity of biological tissue”, Ultrason. Imaging, 13, 111-134, (1991).

[13] B. S. Garra, I. Céspedes, J. Ophir, S. Spratt, R. Zuurbier, C. Magnant and M. Pennanen, "Elastography of breast lesions: initial clinical results." Radiology, 202, 79-86, (1997)

[14]A. Athanasiou, A. Tardivon, M. Tanter, B. Sigal-Zafrani, J. Bercoff, T. Deffieux, J-L. Gennisson, M. Fink and S. Neuenschwander, “Breast lesions: Quantitative elastography with supersonic shear imaging – Preliminary results”, Radiology, 256, 297-303, (2010).

[15] L. Castera, X. Forns and A. Alberti, “Non-invasive evaluation of liver fibrosis using transient elastography”, J. Hepat., 48, 835-847, (2008).

[16] J. Ophir, S. Alam, B. Garra, F. Kallel, E. Konofagou, T. Krouskop and T. Varghese, “Elastography: Ultrasonic estimation and imaging of the elastic properties of tissues”, Proc. Inst. Mech. Eng. Part H.: J. Eng. Medicine, 213, 203-233, (1999).

[17] J. Bercoff, M. Tanter and M. Fink, “Supersonic shear imaging: A new technique for soft tissue elasticity mapping”, IEEE Trans. Ultras. Ferroelec. Freq. Control, 51, 396-409, (2004).

[18] J. Ophir, R. Miller, H. Ponnekanti, I. Céspedes and A. Whittaker, “Elastography of beef muscle”, Meat Science, 36, 239-250, (1994).

[19] S. Catheline, J-L. Gennisson, G. Delon, M. Fink, R. Sinkus, S. Abouelkaram and J. Culioli, “Measuremento of viscoelastic properties of homogeneous soft solid using transient elastography: An inverse problem approach”, J. Acoust. Soc. Am., 116, 3734-3741, (2004).

[20] J-L. Gennisson, S. Catheline, S. Chaffaï and M. Fink, “Transient elastography in anisotropic medium: Application to the measurement of slow and fast shear wave speed in muscles”, J. Acoust. Soc. Am., 114, 536-541, (2003).

[21] A. Ayadi, J. Culioli and S. Abouelkaram, “Sonoelasticity to monitor mechanical changes during rigor and ageing”, Meat Science, 76, 321-326, (2007).

[22] X. Zhang and J. Greenleaf, “Estimation of tissue’s elasticity with surface wave speed”, J. Acoust. Soc. Am., 122, 2522-2525, (2007).

[23] G. Grinspan, S. Aguiar and N. Benech, “Optimization of a surface wave elastography method through diffraction and guided wave effects characterization”, J. Phys: Conference Series, 705, 012014, (2016).

[24] J. Martin, S. Brandon, E. Keuler, J. Hermus, A. Ehlers, D. Segalman, M. Allen and D. Thelen, “Gauging force by tapping tendons”, Nature communications, 9:1592, (2018).

[25] T. Ikeda, P-K. Choi, T. Ishii, I. Arai and M. Osawa, “Firmness evaluation of watermelon flesh by using surface wave elastic waves”, J. Food Eng., 160, 28-33, (2015).

[26] N. Benech, G. Grinspan, S. Aguiar and C. Negreira, “Surface wave elastography: Device and method”, Meas. Sci. and Tech., 30 (3), 035701, (2019).

[27] N. Benech, J. Brum, G. Grinspan, S. Aguiar and C. Negreira, “Analysis of the transient surface wave propagation in soft solids elastic plates”, J. Acoust. Soc. Am., 142, 2919-2932, (2017).

[28] D. Royer and E. Deulesaint, “Elastic waves in solids I: Free and guided propagation”, Springer-Verlag, Berlin, (2002).

[29] N. Benech and R. Piriz, “Study of mechanical properties of vacuum sealed beef samples using surface wave elastography” 2ndIberoamerican Congress on Food Engineering (in Spanish), CIIAL, Punta del Este, Uruguay, (2016).

[30] J. Bercoff, M. Tanter and M. Fink, “Supersonic shear imaging: a new technique for soft tissue elasticity mapping”, IEEE Trans. Ultras. Ferroelec. Freq. Control, 51, 396-409, (2004).

[31] D. G. Altman and J. M. Bland, “Measurement in medicine: The analysis of method comparison studies”, The Statistician, 32, 307-317, (1983).

[32] D. Yates, D. Moore and D. Starnes, “The practice of statistics”, W.H. Freeman & Co. New York, (2008).

[33] Manual de Carnes Bovina y Ovina. Handbook of Uruguayan Meat. Instituto Nacional de Carnes, available at:http://www.inac.uy/innovaportal/v/1852/4/innova.front/manual-de-carnes-bovina-y-ovina , INAC, (2004).

[34] D.W Zinn, C.T. Gaskins, G.L. Gann, and H.B. Hendrick. “Beef muscle tenderness as influenced by days on feed, sex, maturity and anaton1icallocation”. J. Anim. Sci. 31, 307-309, (1970).

[35] F.K. McKeith, D.L. DevoL R.S. Miles. P.J. Bechtel. and T.R. Carr. “Chemical and sensory properties of thirteen major beef muscles”. J. Food Sci. 50, 869-872, (1985)

[36] J.B.Morgan, J.W. Savell, D.S. Hale. R.K. Miller. D.B. Griffin. H.R. Cross and S.D. Shackelford, “National beef tenderness survey”J. Anim. Sci, 69, 3274-3283, (1991).

[37] G. K.Totland and H.Kryvi, “Distribution patterns of muscle fibre types in major muscles of the bull (Bos taurus)”. Anatomy and Embryology, 184, 441450, (1991).

[38] P. Henckel, “Perimortal metabolic events and consequences for meat quality. Proceedings 2nd Dummerstorf Muscle Workshop Muscle Growth and Meat Quality”, Restock, 17-19 May 1995, 77-82, (1995).

[39] F. Kallel and J. Ophir, “A least-squares strain estimator for elastography”, Ultras. Imaging, 19, 195-208, (1997).

[40] M. A. Stuby-Souva, “Tenderness and aging response of beef muscles of different quality grades before and after freezing” (Doctoral dissertation, Oklahoma State University). CHAP. 3, (1994).

[41] C. Schröder and W. Scott Jr., “On the complex conjugate roots of the Rayleigh equation: The leaky surface wave”, J. Acoust. Soc. Am., 110, 2867-2877, (2001).